

Skyrmion Generation by Current

Younghin Tchoe¹ and Jung Hoon Han^{2,3,*}

¹*Department of Physics and Astronomy, Seoul National University, Seoul 151-742, Korea*

²*Department of Physics and BK21 Physics Research Division,
Sungkyunkwan University, Suwon 440-746, Korea*

³*Asia Pacific Center for Theoretical Physics, POSTECH, Pohang, Gyeongbuk 790-784, Korea*

(Dated: July 30, 2018)

Skyrmions, once a hypothesized field-theoretical object believed to describe the nature of elementary particles, became common sightings in recent years among several non-centrosymmetric metallic ferromagnets. For more practical applications of Skyrmionic matter as carriers of information, thus realizing the prospect of “Skyrmionics”, it is necessary to have the means to create and manipulate Skyrmions individually. We show through extensive simulation of the Landau-Lifshitz-Gilbert equation that a circulating current imparted to the metallic chiral ferromagnetic system can create isolated Skyrmionic spin texture without the aid of external magnetic field.

PACS numbers: 73.43.Cd, 72.25.-b, 72.80.-r

I. INTRODUCTION

Skyrmions are topological configurations of a vector order parameter in field-theoretical systems, whose existence had been anticipated mathematically by the particle physicist Tony Skyrme for half a century¹. The two-dimensional version of it, sometimes known as the baby Skyrmion, was recognized to be the topological solution of the non-linear sigma model, which serves as a model for ferromagnets in two dimensions². The discovery of two-dimensional Skyrmions took place in a variety of condensed matter systems such as quantum Hall ferromagnets^{3,4}, metallic chiral ferromagnets⁵⁻⁸, as well as the ferromagnetic monolayer⁹ and doped antiferromagnet¹⁰, and is predicted to be possible in two-dimensional liquid crystal systems¹¹. A series of metallic magnets of B20 structure including MnSi⁵, Fe_{1-x}Co_xSi^{6,7}, and FeGe⁸ is now known to host the Skyrmionic magnetic texture. In these magnetic materials the formation of Skyrmions is a consequence of the competitive interplay between the Dzyaloshinskii-Moriya (DM) interaction which tends to induce magnetic spirals, and an external magnetic field which tends to bring about a ferromagnetic background^{12,13}. Initial theoretical consideration assumed a layered structure of Skyrmions embedded in a three-dimensional crystal and found a small region for its stability just below the magnetic ordering transition temperature^{5,12}. Later, Monte Carlo simulation for two-dimensional magnetic model showed a much wider region for its existence extending down nearly to zero temperature^{7,14}, as was indeed verified in experiment on a thin-film Fe_{0.5}Co_{0.5}Si⁷, due to the lack of competing magnetic structures in the thin-film geometry. Upon increasing the thickness of the film, the Skyrmion phase gradually moves to a higher temperature regime⁸.

Aside from their fundamental scientific allure, it is of importance now to ask if these novel topological objects can be manipulated to the extent that they can be used as carriers of charge, spin, and of information in general. Applying external magnetic field to a chiral ferro-

magnet generates a lattice of Skyrmions, or a Skyrmion crystal⁵⁻⁸. Spin wave fluctuations can be induced in the Skyrmion crystal by applying an additional ac magnetic field as was recently studied theoretically^{15,16}. Other than by magnetic field, the Skyrmions can be manipulated through the Hund’s rule coupling of the spin of electrons in the metallic host to the localized moments forming the Skyrmionic texture. Recent demonstration of the rotation of the Skyrmion crystal axis by the applied current^{17,18} is an example of this kind. In the absence of pinning, Skyrmions are expected to move with the velocity equal to the drift velocity of the electrons responsible for the current¹⁹. Gilbert damping modifies the Skyrmion trajectory in such a way to induce Hall-like motion of Skyrmion orthogonal to the current direction¹⁹.

Although various aspects of current-induced motion of Skyrmions have been studied theoretically in a number of papers already^{18,19}, the possibility of *generating Skyrmions by the current* has not been addressed yet. From a technological point of view, it is desirable to have the extra means to generate and destroy Skyrmions one at a time, instead of having to generate them only in the form of a crystal by the external field. Such possibility, once realized, will help usher the era of “Skyrmionics” - an effort to tailor Skyrmions as carriers of information bits. In this article, using extensive simulation of Landau-Lifshitz-Gilbert (LLG) equation, we provide evidence that circulating spin current can couple to local magnetic moments to produce Skyrmion spin texture in the latter. Basic theory and LLG equation are introduced in Sec. II. Numerical findings are given in Sec. III. Possibility of experimental realization will be discussed in Sec. IV.

II. FORMULATION

We imagine a thin slab of chiral ferromagnet, such that all degrees of freedom behave identically along the thickness direction. The dynamics of the localized moments

\mathbf{n} are governed by the Hamiltonian^{7,19}

$$H_{\mathbf{n}} = \frac{J}{2a} \int d^3\mathbf{r} \sum_{\mu=x,y} (\partial_{\mu}\mathbf{n}) \cdot (\partial_{\mu}\mathbf{n}) + \frac{D}{a^2} \int d^3\mathbf{r} \mathbf{n} \cdot \nabla \times \mathbf{n} - \frac{1}{a^3} \int d^3\mathbf{r} \mathbf{B} \cdot \mathbf{n}. \quad (1)$$

Formulated in the continuum, a expresses the linear dimension of the suitably chosen unit cell, while J and D are the ferromagnetic and DM exchange energies, respectively. The Zeeman field \mathbf{B} is typically applied perpendicular to the planar direction, $\mathbf{B} = B\hat{z}$. The dynamics of the conduction electrons and the coupling of their spins to the local moment, on the other hand, are embodied in the sd Hamiltonian,

$$H_{sd} = \int d^3\mathbf{r} \Psi^\dagger \left(\frac{\mathbf{p}^2}{2m} - J_H \boldsymbol{\sigma} \cdot \mathbf{n} \right) \Psi, \quad \Psi = \begin{pmatrix} c_\uparrow \\ c_\downarrow \end{pmatrix}. \quad (2)$$

Electron operators are given in the spinor form Ψ comprising up (c_\uparrow) and down (c_\downarrow) spin components. Derivation of the subsequent equation of motion of \mathbf{n} based on the total Hamiltonian $H = H_{\mathbf{n}} + H_{sd}$ is well-documented in the literature²⁰ and reproduced briefly here.

In the large Hund's coupling limit ($J_H \rightarrow \infty$) the spin $\Psi^\dagger \boldsymbol{\sigma} \Psi$ of the conduction electron is forced to align with the local magnetization direction \mathbf{n} while the electron band with anti-parallel spins forms a higher-energy continuum. The idea is implemented by making the unitary transformation, $U^\dagger \mathbf{n} \cdot \boldsymbol{\sigma} U = \sigma_z$, where U is given by

$$U = \begin{pmatrix} z_1 & z_2^* \\ z_2 & -z_1^* \end{pmatrix}, \quad z_1 = \cos \frac{\theta}{2}, \quad z_2 = e^{i\phi} \sin \frac{\theta}{2}. \quad (3)$$

The spinor $\mathbf{z} = \begin{pmatrix} z_1 \\ z_2 \end{pmatrix}$ forms the CP^1 representation of the classical spin $\mathbf{n} = \mathbf{z}^\dagger \boldsymbol{\sigma} \mathbf{z} = (\sin \theta \cos \phi, \sin \theta \sin \phi, \cos \theta)$. The new electron spinor $U^\dagger \Psi$ has the upper (lower) component parallel (anti-parallel) to \mathbf{n} , out of which we choose to keep the upper one only, denoted ψ . The field operator ψ gives the electron whose spin direction is projected strictly parallel to the local moment \mathbf{n} . The Hamiltonian for ψ is

$$H'_{sd} = \int d^3\mathbf{r} \psi^\dagger \frac{[\mathbf{p} + \hbar \mathbf{a}]^2}{2m} \psi, \quad (4)$$

where the gauge field \mathbf{a} is derived from \mathbf{z} as $a_i = -i\mathbf{z}^\dagger \partial_i \mathbf{z}$. It is gauge-invariant under $\mathbf{z} \rightarrow e^{i\chi} \mathbf{z}$, and $\psi \rightarrow e^{-i\chi} \psi$. Expanding the sd Hamiltonian gives the coupling of local moment to the electrons as²⁰

$$H_{\mathbf{a}-\mathbf{j}} = \int d^3\mathbf{r} \left(\hbar \mathbf{a} \cdot \mathbf{j} + \frac{\hbar^2 \rho}{2m} \mathbf{a}^2 \right), \quad (5)$$

where we also introduced paramagnetic spin current \mathbf{j} and the spin density ρ as²⁰

$$\mathbf{j} = \frac{1}{2m} (\psi^\dagger [\mathbf{p}\psi] - [\mathbf{p}\psi^\dagger] \psi), \quad \rho = \psi^\dagger \psi. \quad (6)$$

We focus on the dynamics of the local moments using $H_{\mathbf{n}} + H_{\mathbf{a}-\mathbf{j}}$ as the total Hamiltonian and ask how an externally imposed spin current pattern \mathbf{j} influences the magnetic dynamics. Already the likelihood of Skyrmion induction by the circulating \mathbf{j} can be seen in the following simple argument. In a steady state, the divergence of the current vanishes, $\nabla \cdot \mathbf{j} = 0$, making it possible to re-write \mathbf{j} as the curl $\mathbf{j} = \nabla \times \mathbf{c}$. For circulating current of cylindrically symmetric form, the vector field \mathbf{c} is directed in the z -direction. Integrating the energy functional by parts, one can re-write $\mathbf{a} \cdot \mathbf{j} \sim -\mathbf{c} \cdot \nabla \times \mathbf{a}$ and find the effective magnetic field $(\nabla \times \mathbf{a})_z$ couples linearly to the current source \mathbf{c} . This effective magnetic field is nothing other than the Skyrmion density through the relation

$$(\nabla \times \mathbf{a})_z = \frac{1}{2} \mathbf{n} \cdot (\partial_x \mathbf{n} \times \partial_y \mathbf{n}). \quad (7)$$

A suitable \mathbf{c} (\mathbf{j}) of sufficient strength will overcome the nucleation energy cost and induce a Skyrmion with $(\nabla \times \mathbf{a})_z \neq 0$. The sign dictates that the creation of Skyrmion, $Q > 0$, is energetically preferred for counter-clockwise (CCW) direction of spin current, while anti-Skyrmions, $Q < 0$, are preferred for clockwise (CW) spin current direction. Here

$$Q = \frac{1}{4\pi} \int d^2\mathbf{r} \mathbf{n} \cdot (\partial_x \mathbf{n} \times \partial_y \mathbf{n}) \quad (8)$$

is the total Skyrmion charge.

The real-time action for the magnetic dynamics is

$$\frac{\hbar S}{a^3} \int d^3\mathbf{r} dt (1 - \cos \theta) \partial_t \phi - \int dt (H_{\mathbf{n}} + H_{\mathbf{a}-\mathbf{j}}) \quad (9)$$

with the effective moment S , and (θ, ϕ) are the polar and azimuthal angles of the magnetization unit vector \mathbf{n} . The LLG equation follows as

$$\dot{\mathbf{n}} + \frac{1}{\hbar} \mathbf{n} \times (-Ja^2 \nabla^2 \mathbf{n} + 2Da \nabla \times \mathbf{n} - \mathbf{B}) + \alpha \mathbf{n} \times \dot{\mathbf{n}} + \frac{a^3}{S} (\mathbf{j} \cdot \nabla) \mathbf{n} = 0. \quad (10)$$

The Gilbert damping constant α is introduced phenomenologically²⁰. Assuming all the spins sharing the same (x, y) -coordinate behave identically, we arrive at a two-dimensional discretized version of the LLG equation

$$\begin{aligned} \dot{\mathbf{n}}_i + \mathbf{n}_i \times \sum_{j \in i} \left(-\mathbf{n}_{i+a\hat{e}_{ji}} + \kappa \mathbf{n}_{i+a\hat{e}_{ji}} \times \hat{e}_{ji} - \kappa^2 \mathbf{b} \right) \\ + \alpha \mathbf{n}_i \times \dot{\mathbf{n}}_i \\ + \frac{1}{v_0} \left(v_i^x (\mathbf{n}_{i+a\hat{x}} - \mathbf{n}_i) + v_i^y (\mathbf{n}_{i+a\hat{y}} - \mathbf{n}_i) \right) = 0. \end{aligned} \quad (11)$$

The drift velocity $\mathbf{v}_i = (v_i^x, v_i^y)$ is related to the current density through $a^3 \mathbf{j} = px\mathbf{v}$, where x is the number of conduction electrons enclosed in a unit cell of volume a^3 and p is the spin polarization fraction. All physical quantities in the equation are made dimensionless by choosing the unit of time $t_0 = \hbar/J$, and $\kappa = D/J$, $\mathbf{b} = \mathbf{B}/(D^2/J)$. The quantity $v_0 = aS/t_0px$ with the dimension of velocity is introduced as well. The wavelength of the spiral is given by $\lambda \sim 2\pi\sqrt{2}a/\kappa$ in two dimensions. Square lattice of size $L \times L$ is adopted throughout the simulation and the κ value equal to 0.5, which yields the spiral wavelength $\lambda \sim 4\pi\sqrt{2}a \sim 17.8a$. The diameter of the Skyrmion is roughly $\lambda/2$, which makes the Skyrmion radius $R_s \sim \lambda/4$. The sum $\sum_{j \in i}$ spans the four nearest neighbors of the site i , connected by the unit vectors \hat{e}_{ji} .

Time-integration of the discrete LLG equation (11) is done using the fourth-order Runge-Kutta method. Each unit of time t_0 is sliced into over 1000 steps for the integration procedure, with no difference in the result

found for finer step sizes. Typical integration ran up to $t/t_0 \sim 10^3$ without a noticeable error accumulation. The spin current density $\mathbf{j} = \mathbf{v}/v_0$ is given the circulating profile with the Lorentzian shape

$$\mathbf{j}(\mathbf{r}) = \hat{\phi} j_0 \frac{R_c^2}{R_c^2 + r^2} \quad (12)$$

at the center of the simulation lattice, characterized by its magnitude j_0 and the extent R_c . Both positive and negative j_0 corresponding to the CCW (CW) circulation of the spin current were considered. In our convention, a uniform spin current $\mathbf{j} = \mathbf{j}_0$ leads to the Skyrmion flow velocity \mathbf{v}_s in the same direction, $\mathbf{v}_s \parallel \mathbf{j}_0$, opposite to what was used in Ref. 19. Previous study^{7,12,13} found the magnetic phase with helical spin configuration at zero magnetic field and Skyrmion crystal phase over the intermediate field values $b_{c1} \lesssim b \lesssim b_{c2}$. Two magnetic fields are considered in our simulation here, one for b slightly less than the upper critical field strength b_{c2} where a typical ground state consists of ferromagnetic spins dotted with a few isolated anti-Skyrmions (Fig. 1b)^{7,8,13}, and the other at $b = 0$ and having the helical spins as the ground state (Fig. 2b). We refer to these two ground states as FM' (FM+anti-Skyrmions) and H, respectively.

III. PROCESSES OF CURRENT-INDUCED SKYRMION FORMATION

A. Skyrmion production

Due to the simpleness of the ferromagnetic spin background, it is easier to understand the formation process of Skyrmions for the FM' case, $b \lesssim b_{c2}$. For optimal Skyrmion generation condition we choose R_c comparable to the typical radius of a Skyrmion, $R_c \approx R_s$. As the system evolves over time, the time-dependent Skyrmion number $Q(t) = (1/4\pi) \int d^2\mathbf{r} \mathbf{n}(t) \cdot (\partial_x \mathbf{n}(t) \times \partial_y \mathbf{n}(t))$ is evaluated to keep track of the Skyrmion creation process.

As shown in Fig. 1, CW spin current produces, for a brief moment, a spin texture that corresponds roughly to a Skyrmion-anti-Skyrmion pair within the radius $r \lesssim R_s$ (red core region in Fig. 1c-d). Out of the pair, the Skyrmion part soon vanishes, leaving behind an anti-Skyrmion (Fig. 1e-g). The anti-Skyrmion then gradually

drifts out, due to the finite Gilbert damping which gives rise to a velocity orthogonal to the local current flow. The Gilbert damping-induced Skyrmion Hall motion was extensively discussed in Ref. 19 to which we refer the interested readers. The Skyrmion meanwhile experiences an inward flow and vanishes. Once the anti-Skyrmion has drifted a sufficient distance out, another burst of Skyrmion-anti-Skyrmion pair takes place (Fig. 1h), with the Skyrmion portion vanishing through the core again decreasing the total Skyrmion number by an integer amount (Fig. 1i-l). Each burst of the Skyrmion-anti-Skyrmion pair and the subsequent decay of the Skyrmion is responsible for the total Skyrmion number $Q(t)$ jumping by an integer amount as shown in Fig. 1a.

Evidently creation of Skyrmion-anti-Skyrmion pair (Skyrmion dipole) is energetically cheaper than creating an isolated Skyrmion (Skyrmion monopole). Once a pair is created, the Gilbert damping-induced Hall motion naturally moves the two objects in the opposite di-

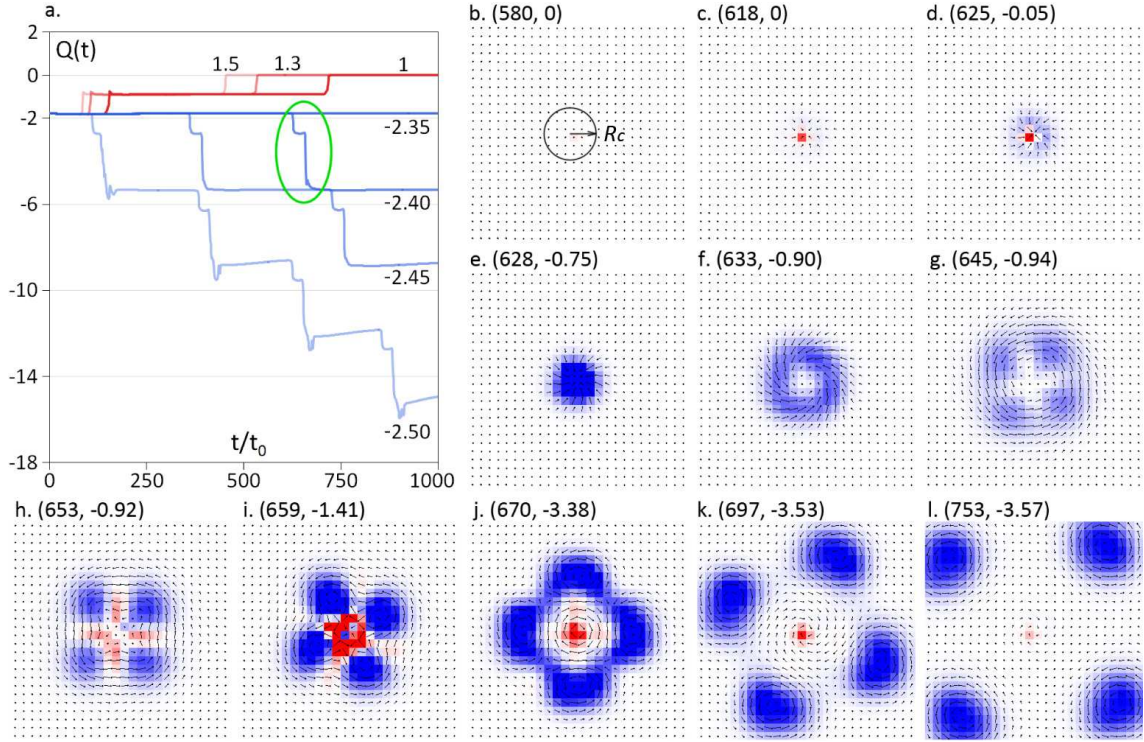


FIG. 1: (color online) Skymion generation by circulating spin current source in the FM' background. (a) Time dependence of the total Skymion number $Q(t)$. $Q(0) \approx -2$ is nonzero from the residual anti-Skymions in the ferromagnetic background. Blue (red)-colored curves correspond to CW (CCW) circulating current with the j_0 value indicated for each curve. (b)-(l) Time-dependent snapshots of the spin configuration over the green-circled time interval in (a). Adjacent spins are separated by the distance a . The circle at the center of (b) indicates R_c , the extent of the current source. Residual anti-Skymions lie outside the field of view. Red and blue refer to positive and negative Skymion densities, respectively. Time at which the snapshot is taken and the change in the Skymion number are given as $(t/t_0, Q(t) - Q(0))$ above each figure. Skymion number is seen to decrease by one, and later by three. Threshold value j_{0c} lies between 2.35 and 2.4 for CW spin current.

rections, so that only one species of Skymions can leave the current core. When CCW current ($j_0 > 0$) is applied, the same Gilbert drifting mechanism that pushed the anti-Skymions out now tends to absorb the nearby anti-Skymions toward the core region because the direction of the Hall motion is also reversed. When an anti-Skymion is pulled sufficiently close to the center, a brief burst of Skymion appears at the core and “eats up” the attracted anti-Skymion. A good mental picture of the process is to take Fig. 1b-1g and reverse them in time. When all the existing anti-Skymions are eaten up in this way, the total Skymion number $Q(t)$ remains close to zero (Fig. 1a) and does not rise above it as a consequence of the fact that positive charge Skymions are energetically forbidden for the magnetic field $b > 0$.

There is a critical value of the spin current density j_{0c} required to produce anti-Skymions out of the ferromagnetic spin background. Obviously the rate of energy input from the circulating current needs to outpace that of the energy drain due to the Gilbert damping in order to supply sufficient energy to create an anti-Skymion. Above the threshold, $|j_0| > j_{0c}$, the total Skymion number begins to jump in integer steps with time intervals that decrease as $|j_0| - j_{0c}$ increases (Fig. 1a).

Figure 2 depicts the Skymion creation process for H background ($b = 0$). As with the FM' background, $Q(t)$ can be seen to increase in integer quantized steps. In contrast to $b > 0$ case which prefers an anti-Skymion charge, opposite signs of the circular current result in more or less symmetrical profiles of $Q(t)$ as shown in Fig. 2a. Snapshots of spin configurations for $Q = 0 \rightarrow Q = 1$ are in Fig. 2b-g, and those of $Q = 1 \rightarrow Q = 2$ in Fig. 2h-l. At first a small patch of helical spin is torn into two disjoint segments as in Fig. 2c-d near the current core, giving way to the nucleation of some defects in the intervening region. The defect profile is best described as the meron-anti-Skymion-meron composite (merons are in blue, anti-Skymion in red in Fig. 2c), out of which the central anti-Skymion shrinks in size while the two merons drift out, again due to the Gilbert damping-induced Hall motion. The two merons are responsible for the total charge $Q(t) \approx 1$. Each time the process repeats itself, the Skymion number increases by one.

In both H and FM' spin backgrounds, the resulting charge of the Skymions produced by the current is correlated with the helicity of the circulation as predicted in an earlier argument; see paragraph following Eq. (6). In detail, however, the production process proves to be

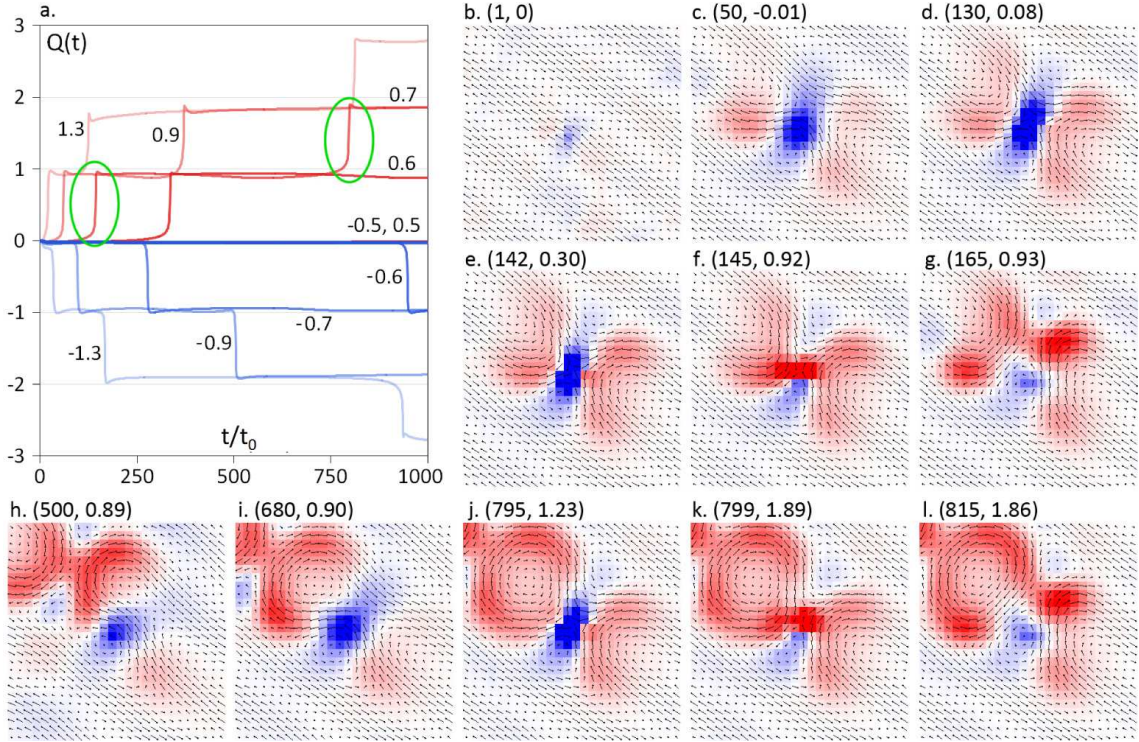


FIG. 2: (color online) Skyrmion generation by circulating spin current source in the H background. (a) Time dependence of the total Skyrmion number $Q(t)$ for various j_0 values. Initial Skyrmion number is zero for the helical spin. Same color convention as in Fig. 1 applies throughout this figure. (b)-(l) Two sets of snapshots corresponding to $Q = 0 \rightarrow 1$ and $Q = 1 \rightarrow 2$ corresponding to two green circles in Fig. 2a.

far more intricate involving an Skyrmion-anti-Skyrmion pair at the initial stage of metamorphosis rather than the simple creation of an isolated Skyrmion out of the vacuum. A different mechanism then intervenes, namely Gilbert damping-assisted Hall motion, which separates the pair according to their respective charges, leaving only one species of Skyrmions to survive at the end.

B. Influence of Gilbert damping

Gilbert damping plays a major role in the generation of Skyrmions and anti-Skyrmions by facilitating their radially outward motion from the circulating spin current region. All results shown in Figures 1 and 2 are obtained for $\alpha = 1$, which is a fairly large value for Gilbert damping parameter. As the damping is reduced, the sharp, integer quantization of Skyrmion number $Q(t)$ gets less conspicuous as shown in Fig. 3. According to our numerical observation, clear integer quantization of $Q(t)$ is more or less synonymous with the production of well-isolated Skyrmions in real space, which only becomes possible for α in excess of certain minimum value as shown in Fig. 3b and 3d. This is related to the quite complex manner in which the Skyrmion creation process takes place. The initial creation process, as shown in Figs. 1 and 2, always

involves a pair of Skyrmions of opposite charges, out of which only one is pushed outwards by virtue of Gilbert damping-assisted Hall motion. A large Hall motion requires a correspondingly large Gilbert damping constant. Otherwise, when α is small, those Skyrmions after generation continue to move in circular path (because current is circular) rather than drifting out, and collide/merge with other Skyrmions. This leads to a large overlap between spatially adjacent Skyrmions, as well as a non-integral value of $Q(t)$ ²². Only with sufficiently large α do we find that the Skyrmions are being pushed out fast enough after their generation to minimize the overlap and give rise to integer $Q(t)$. Mochizuki's recent LLG simulation¹⁶ uses the Gilbert constant $\alpha \leq 0.04$, while extra damping effects due to spin-motive force are expected to increase this value to around 0.1¹⁹. Further enhancing the Gilbert damping might require intentional disordering of the film by irradiation.

C. Skyrmion lifetime

Once the Skyrmions have been generated by means of current, it is important that they remain there after the current is turned off if they are to serve as memory bits. After the current was applied long enough to nucleate a Skyrmion, we turned it off in the simulation to see if it

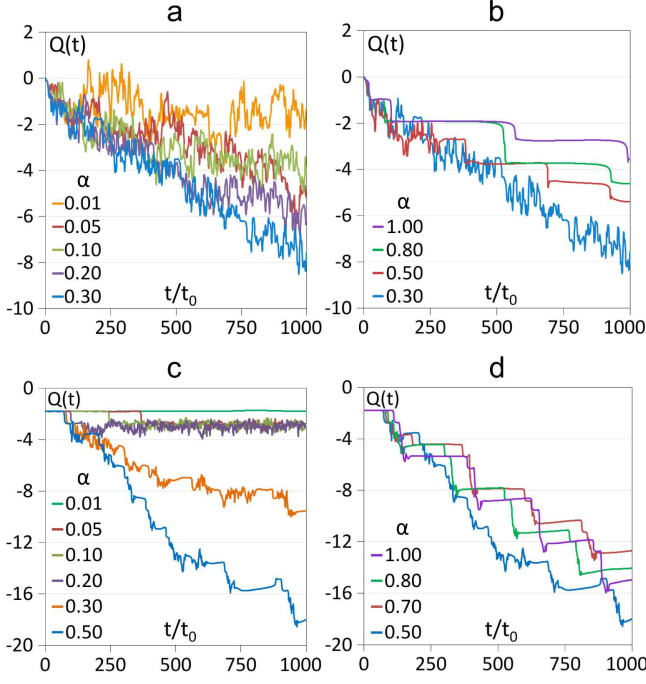


FIG. 3: (color online) Influence of Gilbert damping on Skymion generation. (a)-(b) Plot of Skymion number $Q(t)$ with $b = 0$ (H background) for different Gilbert damping constants α . $|Q(t)|$ increases monotonically with α without showing signs of quantization when α is small. At a larger damping, $0.3 < \alpha < 0.5$, quantization of Skymion number begins to occur. The time span of each integer plateau becomes longer, and the production rate of Skymions becomes less, with increasing α . (c)-(d) Plot of the Skymion number $Q(t)$ with FM' background. Numbers in the inset are the Gilbert damping constants. $(j_0, R_c) = (-1.5, 3.0)$ was used for (a)-(b) and $(j_0, R_c) = (-2.5, 3.0)$ for (c)-(d).

would decay. In fact, the decay of Skymion is expected because without the current, the Skymion would be in a metastable state. As the $Q(t)$ plots in Fig. 4b and 4d show, however, the anti-Skymions once created remain extremely stable although energetically it cannot exist in the ground state for $b = 0$. As far as our numerical simulation lasts, the spin patterns shown in Fig. 4a and 4c remained persistently the same. Such a long lifetime of an isolated Skymion is a positive feature in utilizing the chiral ferromagnet as a platform for encoding Skymion-based information.

D. Effects of radial current pulse

Earlier we used the circulating current as a platform to generate Skymions electrically. Clear, integer quantization of Skymion charge was possible only for very large Gilbert damping parameters. Here we show that Skymions can also be created by radial current pulses as given by

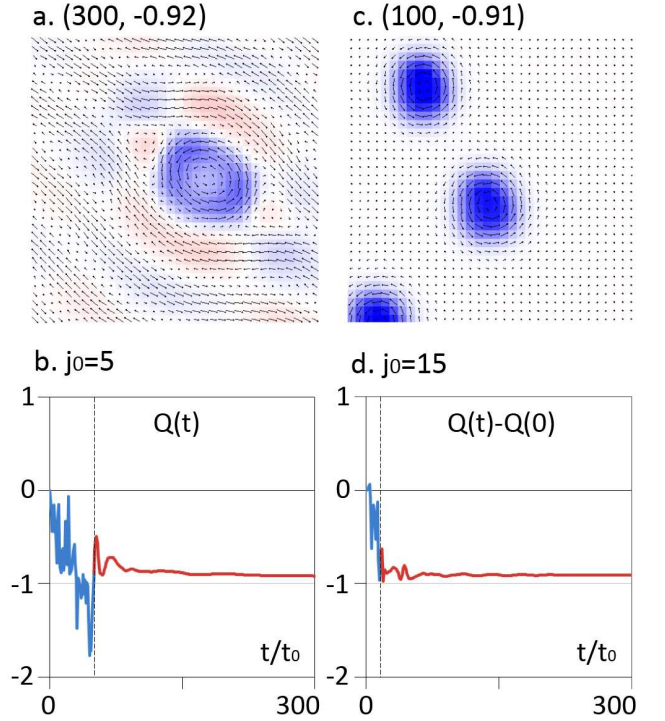


FIG. 4: (color online) Skymion generation by pulse current. (a)-(b) Pulse current of size $j_0 = 5$ is applied for $0 < t_1/t_0 < 50$ over the helical spin state and then turned off. (c)-(d) $j_0 = 15$ for $0 < t_1/t_0 < 15$ over the FM' state. Dotted vertical line in (b) and (d) indicates the termination of the applied current. Top row: the spin configuration and Skymion number $Q(t) - Q(0)$ when a sufficiently long time has elapsed after the current is turned off. Bottom row: time dependence of the Skymion number $Q(t) - Q(0)$. All current directions are CCW with $R_c = 3$ and $\alpha = 0.1$.

$$\mathbf{j}(\mathbf{r}) = \hat{r} \frac{j_0}{\sqrt{2}r}. \quad (13)$$

While the radial current source remains on, a bunch of plus and minus Skymion fragments appear from the center and drift out as they collide and annihilate with oppositely charged fragments as shown in Fig. 5a. When the radial current is turned off, most of the plus and minus Skymion fragments annihilate, leaving behind a portion that evolves into an integer-valued Skymion, with the sign as favored by the direction of the applied magnetic field, as shown in Fig. 5b and 5c. This way of creating Skymion is only possible when external magnetic field is acting on the helical magnet. For helical spin configuration, the plus and minus Skymion densities created by the radial current annihilate and disappear completely, returning back to the initial helical spin configuration over time.

We emphasize that this method of generating Skymions in the FM' background works very well even for small values of the Gilbert damping constant α . This is because the selection process to isolate one particular

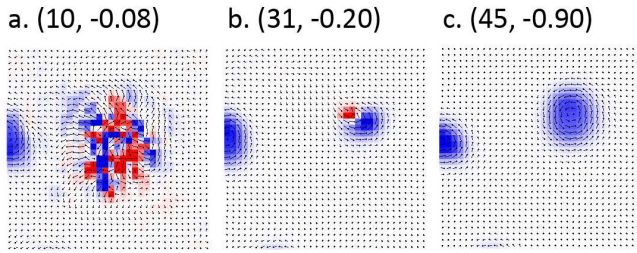


FIG. 5: (color online) Skyrmion creation by radial current source. Current pulse with $j_0 = 10$ lasting for $t/t_0 = 10$ was given. The numbers above each figure indicate $(t/t_0, Q(t) - Q(0))$. (a) Right at the turn-off, one finds a swarm of positive and negative Skyrmion fragments. (b) After some time has passed, most of the Skyrmions and anti-Skyrmions have annihilated each other, leaving behind a predominant anti-Skyrmion density due to the external magnetic field. (c) Final state shows one anti-Skyrmion.

sign of Skyrmion is done by external magnetic field, not by Gilbert damping as in the case of circulating current.

IV. EXPERIMENTAL REALIZATION AND DISCUSSION

The typical exchange energy scale of a chiral ferromagnet is $J_0 \sim 3$ meV²³, with the dispersion $\hbar\omega_k \sim J_0(ka_0)^2$ involving a_0 , the linear dimension of the physical unit cell. On the other hand, from our continuum LLG equation in (10) follows the dispersion relation $\hbar\omega_k \sim J(ka)^2$. Hence, J used in our model is related to the microscopic parameter J_0 by $J \sim J_0(a_0/a)^2$, which also sets the time and the velocity scales as $t_0 = \hbar/J \approx 220(a/a_0)^2$ fs and $v_0 = aS/t_0px \sim (a_0J_0/\hbar)(S/p)(a_0/a)^4 \sim 1.8 \times 10^3(S/p)(a_0/a)^4$ m/s.

In order to fix the ratio a/a_0 , we note that with our choice $\kappa = 0.5$ the typical wavelength of the spiral is $\lambda = 4\pi\sqrt{2}a \approx 17.8a$. Values of λ vary quite markedly among the chiral ferromagnets, ranging from ~ 3 nm for FeGe²¹, ~ 20 nm for MnSi⁵, ~ 70 nm for FeGe⁸, and ~ 90 nm for Fe_{1-x}Co_xSi^{6,7}. Taking the characteristic spiral wavelength $\lambda \sim 60$ nm yields $17.8a \sim 60$ nm, or $a \sim 4$ nm. Choosing the microscopic lattice constant $a_0 = 4\text{\AA}$ then gives the ratio $a/a_0 \sim 10$. Finally, with

the spin polarization fraction $p \sim 0.1$ and $S = 1$ we obtain $v_0 \sim 1$ m/s. The critical current density j_{0c} of order unity we saw in the simulation thus corresponds to the drift velocity of a few m/s to be imparted to the conduction electrons. Estimate of the carrier concentration in MnSi²⁴ $\rho_e \sim 10^{28} - 10^{29}/\text{m}^3$ yields the critical current density $j_c \sim 10^{10} - 10^{11}\text{A}/\text{m}^2$, which is close to, or below the critical current required for domain wall switching in typical magnetic devices²⁰. The time interval between successive Skyrmion creation events as shown in Figs. 1 and 2 is $\sim 100t_0$. With the estimate $t_0 \sim 20$ ps, the time interval is ~ 2 ns. The requirement for Skyrmion nucleation is reduced to having a strong current pulse of a few nanosecond duration with the density $j_c \sim 10^{10} - 10^{11}\text{A}/\text{m}^2$ - a practice readily available in modern-day spintronics laboratories.

Although a detailed practical scheme to implement the circuitry needed for the Skyrmion generation is yet to be worked out, our simulation provides a proof-of-concept demonstration for Skyrmion creation by electrical current. It is conceivable, in principle, that an artificial bend in the current pathway (like a curved freeway) is fabricated to mimic the circular pattern we assumed in the simulation. As the current of enough intensity passes through such a bend, Skyrmions will “pop out” from the point of greatest curvature. The Skyrmion production by means of radial current discussed in Sec. III D can be mimicked by designing a narrow channel of metallic magnet that opens up into a much wider region. A current coming through such constriction will be a source of radial motion, thus of Skyrmions. Although much engineering ideas need to be carved out yet, the fundamental processes revealed by the present numerical simulation will be exciting to realize in laboratories in the near future.

Acknowledgments

This work is supported by Mid-career Researcher Program (No. 2010-0008529). Valuable comments on the manuscript from Suk-Bong Choe and discussions with Hyun-Woo Lee are acknowledged. We also thank professor Naoto Nagaosa for careful reading of the initial manuscript and suggestions.

* Electronic address: hanjh@skku.edu

¹ T. H. R. Skyrme, Proc. Roy. Soc. of London, Ser. A **260**, 127 (1961); Nucl. Phys. **31**, 556 (1961).

² R. Rajaraman, *Solitons and Instantons* (North-Holland, 1989).

³ S. L. Sondhi, A. Karlhede, S. A. Kivelson, and E. H. Rezayi, Phys. Rev. B **47**, 16419 (1993).

⁴ S. E. Barrett, G. Dabbagh, L. N. Pfeiffer, K. W. West, and R. Tycko, Phys. Rev. Lett. **74**, 5112 (1995).

⁵ S. Mühlbauer, B. Binz, F. Jonietz, C. Pfleiderer, A. Rosch,

A. Neubauer, R. Georgii, and P. Böni, Science **323**, 915 (2009).

⁶ W. Münzer, A. Neubauer, T. Adams, S. Mühlbauer, C. Franz, F. Jonietz, R. Georgii, P. Böni, B. Pedersen, M. Schmidt, A. Rosch, and C. Pfleiderer, Phys. Rev. B **81**, 041203(R) (2010).

⁷ X. Z. Yu, Y. Onose, N. Kanazawa, J. H. Park, J. H. Han, Y. Matsui, N. Nagaosa, and Y. Tokura, Nature **465**, 901 (2010).

⁸ X. Z. Yu, N. Kanazawa, Y. Onose, K. Kimoto, W. Z.

- Zhang, S. Ishiwata, Y. Matsui, and Y. Tokura, *Nature Mat.* **10**, 106 (2011).
- ⁹ S. Heinze, K. von Bergmann, M. Menzel, J. Brede, A. Kubetzka, R. Wiesendanger, G. Bihlmayer, and S. Blügel, *Nature Phys.* **7**, 713 (2011).
- ¹⁰ I. Raicević, Dragana Popović, C. Panagopoulos, L. Benfatto, M. B. Silva Neto, E. S. Choi, and T. Sasagawa, *Phys. Rev. Lett.* **106**, 227206 (2011).
- ¹¹ J.-i. Fukuda and S. Zumer, *Nature Commun.* doi:10.1038/ncomms1250 (2011).
- ¹² A. N. Bogdanov and D. A. Yablonskii, *Sov. Phys. JETP* **68**, 101 (1989); A. Bogdanov and A. Hubert, *J. Magn. Magn. Mater.* **138**, 255 (1994).
- ¹³ Jung Hoon Han, Jiadong Zang, Zhihua Yang, Jin-Hong Park, and Naoto Nagaosa, *Phys. Rev. B* **82**, 094429 (2010).
- ¹⁴ Su Do Yi, Shigeki Onoda, Naoto Nagaosa, and Jung Hoon Han, *Phys. Rev. B* **80**, 054416 (2009).
- ¹⁵ Olga Petrova and Oleg Tchernyshyov, *Phys. Rev. B* **84**, 214433 (2011).
- ¹⁶ Masahito Mochizuki, *Phys. Rev. Lett.* **108**, 017601 (2012).
- ¹⁷ F. Jonietz, S. Mühlbauer, C. Pfleiderer, A. Neubauer, W. Münzer, A. Bauer, T. Adams, R. Georgii, P. Böni, R. A. Duine, K. Everschor, M. Garst, and A. Rosch, *Science* **330**, 1648 (2010).
- ¹⁸ K. Everschor, M. Garst, R. A. Duine, and A. Rosch, *Phys. Rev. B* **84**, 064401 (2011).
- ¹⁹ J. Zang, M. Mostovoy, J. H. Han, and N. Nagaosa, *Phys. Rev. Lett.* **107**, 136804 (2011).
- ²⁰ G. Tatara, H. Kohno, and J. Shibata, *Phys. Rep.* **468**, 213 (2008).
- ²¹ N. Kanazawa, Y. Onose, T. Arima, D. Okuyama, K. Ohoyama, S. Wakimoto, K. Kakurai, S. Ishiwata, and Y. Tokura, *Phys. Rev. Lett.* **106**, 156603 (2011).
- ²² In a continuum theory one should obtain integer $Q(t)$ even for overlapping Skyrmions. The non-integral values are a result of the calculation being carried out on a discrete lattice.
- ²³ S. V. Grigoriev, S. V. Maleyev, A. I. Okorokov, Yu. O. Chetverikov, P. Böni, R. Georgii, D. Lamago, H. Eckerlebe, and K. Pranzas, *Phys. Rev. B* **74**, 214414 (2006).
- ²⁴ M. Lee, Y. Onose, Y. Tokura, and N. P. Ong, *Phys. Rev. B* **75**, 172403 (2007).